PAPER

The selective recognition mechanism of a novel highly hydrophobic ion-imprinted polymer towards Cd(II) and its application in edible vegetable oil

Hui Cao,† Pu Yang,† Tai Ye, [ID] Min Yuan, Jinsong Yu, Xiuxiu Wu, Fengqin Yin, Yan Li and Fei Xu [ID]*

Edible vegetable oils are easily contaminated by heavy metals, resulting in the oxidative degradation of oils and various health effects on humans. Therefore, it is very important to develop a rapid and efficient method to extract trace heavy metals from vegetable oils. In this work, a highly hydrophobic ion-imprinted polymer (IIP) was synthesized on a novel raspberry (RS)-like particle surface. The synthesized IIP@RS was characterized and used in solid-phase extraction (SPE) for the selective and fast adsorption of Cd(II) from vegetable oils. The results showed that IIP was successfully coated onto RS particles with a high specific surface area (458.7 m² g⁻¹) and uniform porous structure. The contact angle (θ) value (141.8°) of IIP@RS was close to the critical value of super-hydrophobic materials, which is beneficial to their adsorption in hydrophobic vegetable oils. The IIP@RS also exhibited excellent adsorption ability and selectivity to Cd(II) with a maximum adsorption capacity of 36.62 mg g⁻¹, imprinting factor of 4.31 and equilibrium adsorption rate of 30 min. According to isothermal titration calorimetry results, the recognition behavior of IIP@RS for Cd(II) was mainly contributed by Cd(II)-induced cavities during gel formation and coordination between Cd(II) and −SH groups in imprinted cavities. Furthermore, the adsorption process driven by entropy and enthalpy was spontaneous at all temperatures. In real vegetable oil samples, IIP@RS-SPE adsorbed approximately 96.5–115.8% of Cd(II) with a detection limit of 0.62 μg L⁻¹. Therefore, IIP@RS has wide application prospects in enriching and detecting Cd(II) from vegetable oil.

1 Introduction

Edible vegetable oils play a crucial role in human nutrition due to their cholesterol-lowering effect.[1] However, vegetable oils are easily contaminated by trace heavy metals that originate from fertilizers, soil and environmental exposure.[2] These trace heavy metals could promote the oxidative degradation of fatty acids in vegetable oil and decrease their nutritional value.[3] Moreover, heavy metals, such as cadmium, are easily accumulated in the human body through the food chain and lead to various health defects in humans, including stomach aches, vomiting, cell damage and cancer, and weakening the immune system.[4,5] To avoid these adverse effects, the World Health Organization has suggested a very low permissible limit (3 μg L⁻¹) for cadmium ions in environmental samples. Thus, it is important to develop a sensitive analytical method to determine trace cadmium in vegetable oils.

Atomic spectroscopic is the most commonly used technology for determining trace heavy metals.[6,7] However, the direct

School of Medical Instrument and Food Engineering, Shanghai Engineering Research Center for Food Rapid Detection, University of Shanghai for Science and Technology, P. O. Box 454, No. 516, Jungong Road, Shanghai 200093, P. R. China. E-mail: xufei8135@126.com; Fax: +86-21-55271117; Tel: +86-21-55271117

† These authors contributed equally to this work.

measurement of heavy metals in edible vegetable oils by atomic spectroscopic is particularly difficult due to their high viscosity and organic content properties. Many sample pre-treatment methods have been developed to extract heavy metals from vegetable oils, such as the dilution of edible oils with an organic solvent,[8] liquid–liquid extraction,[9] and solid-phase extraction (SPE).[10] Among these methods, SPE is one of the most effective ways because of its low cost, rapidity, simplicity, and ability to combine with different detection techniques.[11] Although SPE has exhibited superior potential for heavy metal adsorption, selectivity remains limited. Therefore, adsorption materials with high selectivity need to be developed to extract trace target ions from complicated vegetable oil samples.

The ion-imprinted polymers (IIPs) have gained considerable attention as sorbents due to their high selectivity and durability against harsh chemical environments. It is commonly prepared by imprinting the target ions in a polymer network followed by removing the template ions to give permanent cavities that are complementary to sizes and shapes of the template ions.[12,13] As a derived technique, IIPs have displayed a considerable potential for selective extraction and recovery of the template ions from complicated vegetable oil samples. However, conventional methods of manufacturing IIPs such as bulk and precipitation polymerization can cause many recognition sites that are deeply

embedded in the inner material, which results in difficulty in recognizing the target ions and challenges in elution because of the diffusion barrier.[14,15] The surface imprinting technique has been used to overcome these disadvantages by immobilizing a thin layer of IIP on the surface of the support materials. Since the recognition cavities are at or close to the surface of the solid particles, the mass transfer resistance of target ions is significantly reduced, which is beneficial to the elution and recombination of template ions. Silica gel particles are commonly used as a support matrix in surface imprinting technologies because they are non-swelling material and the recognition cavities on its surface are more stable. However, it is a challenge to fabricate many recognition cavities on the rigid silica particles.

Raspberry-like (RS) silica particles with a large central microspheres surrounded by many small nanospheres have gained increasing attention as a novel adsorbent due to their high surface area, unique morphology, and excellent structural stability.[16,17] Moreover, RS particles with regular dual-sized hierarchical surface roughness are also ideal supports for the construction of high hydrophobic surface materials, which is beneficial in adsorption and their dispersion in a more hydrophobic environment such as vegetable oils.[18] Therefore, RS particles functioned with IIPs combine the advantages of the large surface area originating from RS particles and selectivity originating from IIPs. However, there have been few reports on the functionalization of RS particles with IIPs, especially for the adsorption of cadmium from vegetable oil samples. There is also a lack of systematic and in-depth study on the mechanism of IIPs binding to target cadmium.

Therefore, in this study, high hydrophobic IIPs were prepared on the surface of the RS carrier using a one-pot sol–gel process. The synthesized IIP@RS was then characterized and used in an SPE system for the extraction of cadmium from vegetable oil samples. Additionally, the mechanism of IIP@RS binding to Cd(II) was investigated by ITC analysis.

2 Materials and methods

2.1 Materials

Vegetable oils were purchased directly from the local supermarket (Shanghai, China). Cadmium chloride ($CdCl_2$) and epichlorohydrin were obtained from Shanghai Aladdin Reagent Company. (3-Mercaptopropyl)trimethoxysilane (MPTMS), cetyltrimethylammonium bromide, tetraethoxysilane (TMOS), and poly(vinyl alcohol) were obtained from Sigma Chemical (Milwaukee, WI, USA). Other reagents were purchased from Sinopharm Chemical Reagent Co., Ltd. (Shanghai, China).

2.2 Preparation of IIP@RS

RS particles were synthesized by a one-step sol–gel process. Briefly, 1 g of cetyltrimethylammonium bromide and 3.75 g of poly(vinyl alcohol) were dispersed in 55 mL of deionized water. Then, 20 mL of ammonia solution (1.4%), 80 mL of methanol, and 5 mmol of MPTMS were dissolved in the above solution and continuously stirred for 24 h at ambient temperature. The resultant microspheres were washed twice with methanol and recovered by centrifugation at 5000 rpm for 10 min. The product was further dried for 8 h at 60 °C and then calcined at 600 °C for 5 h, followed by activation in 33% methanesulfonic acid solution.

IIP@RS was prepared using RS particles as a supporting matrix (Fig. 1). First, 400 nmol of MPTMS and 100 nmol of $CdCl_2$ were dissolved in 50 mL methanol under stirring. Then, 500 mg of activated RS and 400 μL of deionized water were
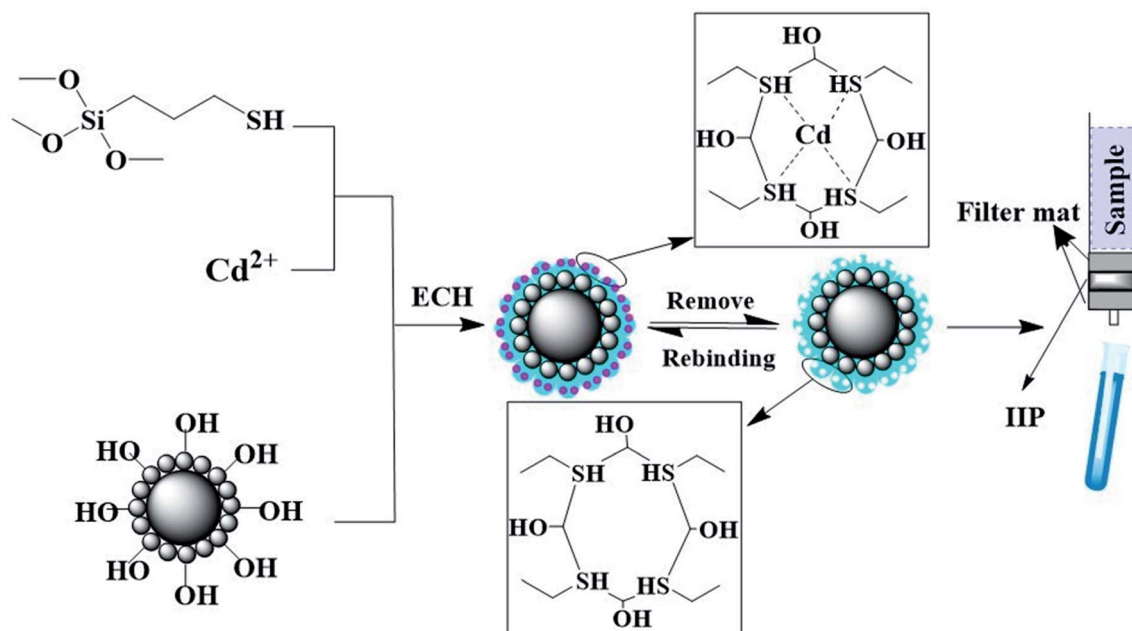

Fig. 1 Schematic of the synthesis procedure of IIP@RS.

dispersed in the above reaction solution and continuously stirred at 80 °C for 24 h. After the reaction temperature was reduced to 50 °C, 400 nmol of epichlorohydrin as a cross-linker was added under stirring for another 2 h. The synthesized polymer powder was washed with 6 mol L^{-1} HCl to remove the template and non-polymerized compounds. The non-imprinted polymer (NIP@RS) was prepared with a similar procedure but without the template ions.

2.3 Characterization of IIP@RS

The content of Cd(II) in the samples was measured using flame atomic absorption spectrometry (FAAS, GBC Scientific Instruments, Australia) equipped with a deuterium lamp background correction system, a cadmium hollow cathode lamp with the wavelength of 228.8 nm and a slit bandwidth of 0.2 nm, and an air acetylene flame. The morphology of RS and IIP@RS was observed by transmission electron microscopy (TEM, FEI Inspect F50, USA). Nitrogen adsorption–desorption isotherms of IIP@RS were determined using a QuadraSorb EVO analyzer (Quantachrome Instruments, USA). The specific surface areas of IIP@RS were calculated from the Brunauer–Emmett–Teller equation using the adsorption data. The size of pores was calculated using the Barrett–Joyner–Halenda equation. The contact angles of IIP@RS were measured using a Dataphysics OCA-20 contact angle analyzer (Dataphysics Inc, Germany) using the sessile drop method. The elemental composition of RS particles and IIP@RS was investigated by X-ray photoelectron spectroscopy (XPS, Smartlab9X, Japan).

2.4 The adsorption characteristics of IIP@RS

In the adsorption isotherm experiment, IIP@RS or NIP@RS (10 mg) was dispersed in 5 mL of Cd(II) solution in the concentration range of 10–500 mg L^{-1}. The mixture was stirred at 25 °C for 30 min, followed by centrifugation at 8000 rpm for 15 min. The content of Cd(II) in the supernatant was measured using FAAS. The adsorption capacity of IIP@RS or NIP@RS toward Cd(II) was further calculated according to the difference between initial and equilibrium concentrations of Cd(II) in the solution and then fitted by Langmuir (eqn (1)) and Freundlich isotherm constants (eqn (2)) (Kong *et al.*, 2018).

$$q_e = \frac{q_{max} b C_e}{(1 + b C_e)} \tag{1}$$

$$q_e = K_F C_e^{1/n} \tag{2}$$

Here, q_e is the amount of the adsorbed Cd(II) in IIP@RS or NIP@RS (mg g^{-1}), C_e is the equilibrium concentration of Cd(II) in the solution (mg L^{-1}), b is the Langmuir constant (L mg^{-1}), and q_{max} is the maximum adsorption capacity (mg g^{-1}). K_F and n are Freundlich constants.

In the adsorption kinetics experiment, IIP@RS (10 mg) was mixed with 5 mL of Cd(II) solution at a 50 mg L^{-1} concentration and stirred at different times (5–150 min) at 25 °C. The adsorption capacity was determined at each time interval and

fitted using a pseudo-first-order model (eqn (3)) and pseudo-second-order model (eqn (4)).[19]

$$\ln(1 - F) = k_a t \tag{3}$$

$$\frac{t}{Q_t} = \frac{1}{k_b Q_e^2} + \frac{1}{Q_e} \tag{4}$$

Here, t represents the time to reach adsorption equilibrium, F equals to Q_t/Q_e represents the adsorption amount of polymers at time t and at equilibrium, k_a and k_b represent the rate constants of adsorption.

In the adsorption selectivity experiment, IIP@RS (10 mg) was added to a 50 mL test tube containing aqueous solutions of Cd(II), Cu(II), Ni(II), Pb(II), and Cr(II) ions at a concentration of 50 mg L^{-1} and stirred at 25 °C for 30 min. Then, the selectivity factor (β) and imprinting factor (α) for Cd(II) ions relative to competing ions were obtained according to the following equations:

$$\alpha = \frac{Q_a}{Q_b} \tag{5}$$

$$\beta = \frac{\alpha_1}{\alpha_2} \tag{6}$$

Here, Q_a and Q_b represent the adsorption capacity of Cd(II) and competing ions (Cu(II), Pb(II), Cr(II), and Ni(II)) onto IIP@RS and NIP@RS, respectively. α_1 and α_2 represent the imprinting factor of Cd(II) ions and competing ions, respectively.

The effect of the solvent type on the adsorption capacity of IIP@RS was investigated. Briefly, IIP@RS or NIP@RS (10 mg) was dispersed in 5 mL of Cd(II) solution with different solvent types (double distilled water, ethanol and methanol) at a concentration of 50 mg L^{-1}. The mixture was stirred at 25 °C for 30 min, followed by centrifugation at 8000 rpm for 15 min. Then, the content of Cd(II) in the supernatant was determined by FAAS.

2.5 Determination of Cd(II) content in edible vegetable oils

IIP@RS particles (30 mg) were loaded into an empty column for the extraction and preconcentration of Cd(II) from vegetable oils. The obtained IIP@RS-SPE column was washed twice using methanol and deionized water to remove the impurities. The sunflower seed oil, soybean oil, olive oil, and corn oil samples from the supermarket were spiked with Cd(II) at the concentration of 2 and 10 mg L^{-1}, and mixed with 1 mL of Triton X-100 to improve the dispersion of Cd(II) in the vegetable oil. Subsequently, the mixture solution was permitted to flow through the IIP@IR-SPE system at a flow rate of 1 mL min^{-1}. The retained Cd(II) in the IIP@IR-SPE system was further eluted using 3 mol L^{-1} of HCl at a flow rate of 1 mL min^{-1} and then determined by FAAS.

2.6 The thiol quantification

Functional monomer MPTMS was grafted onto the RS particle surface to obtain thiol functionalized RS particles (RS-SH). Briefly, 100 mg of RS particles and 1 mL of MPTMS were dispersed in 30 mL of anhydrous toluene and then stirred at 120 °C for 20 h. The white solid products were recovered and

dried at 65 °C for 10 h. Subsequently, the content of free thiol groups in IIP@RS, NIP@RS, and RS-SH was determined according to a modified Ellman method.[20]

2.7 ITC measurement of IIP@RS binding to Cd(ɪɪ)

The mechanism of Cd(ɪɪ) adsorbed by IIP@RS was investigated by ITC calorimeter (GE MicroCal VP-ITC, UK). Briefly, IIP@RS or NIP@RS was dispersed in methanol and titrated using 0.5 mM of $CdCl_2$ solution. The titration speed was set at 370 rpm min^{-1}, and the titration temperature was maintained at 25 °C at a rate of 120 s per drop. The background of the titration curve was subtracted using methanol to titrate the adsorbent under identical titrating conditions.

3 Results and discussion

3.1 Characterization of IIP@RS

3.1.1 XPS analysis.
XPS was used to determine the elemental composition of RS and IIP@RS particles. As shown in Fig. 2a, RS particles were mainly composed of C, O, and Si with peaks at 285 eV, 532 eV, and 103 eV, respectively, derived from the addition of MPTMS. Notably, elemental S was not detected in RS particles, which may be due to the destruction of thiol groups during the calcination process at 600 °C. After the polymerization of template ion and functional monomer MPTMS *via* cross-linking, the two typical peaks appearing at 162 eV and 228 eV attributed to the C–S bonds (thiols) demonstrated that MPTMS molecules were successfully grafted onto the RS particles. Furthermore, C and Si atom percentages of IIP@RS were much higher than those in RS particles, further confirming that MPTMS was successfully cross-linked into the network structure of the imprinted polymer.

3.1.2 Nitrogen adsorption–desorption measurement.
The porosity of IIP@RS was investigated *via* nitrogen adsorption–desorption measurements. It was found that IIP@RS exhibited a typical "type IV" curve with a clear H_1 hysteresis loop within a relative pressure (P/P_0) of 0–0.3 (Fig. 2b), demonstrating that the obtained adsorption materials had highly porous structures with good pore connectivity.[21,22] The specific surface area, and pore diameters, and total pore volumes in IIP@RS samples were further calculated by Brunauer–Emmett–Teller and Barrett–

Joyner–Halenda models, respectively. It was found that the specific surface area of IIP@RS obtained from the nitrogen isotherm was 458.7 m^2 g^{-1} with a total pore volume of 0.31 cm^3 g^{-1}. The pore diameter—calculated according to the adsorption branch of the isotherm—was approximately 2.14 nm with a uniform porous distribution (Fig. 2b, inset).

3.1.3 TEM analysis.
The morphology of IIP@RS and NIP@RS was observed by TEM. As shown in Fig. 3a, nanoparticles with diameters of ∼215 nm were uniformly assembled onto the surface of the microsphere core (∼2.55 μm), confirming the successful synthesis of particles with a typical raspberry-like structure. In the following imprinting polymerization process, a layer of IIP was coated onto the surface of RS particles, resulting in a rough and irregular surface (Fig. 3b). The dual-sized hierarchical surface roughness of IIP@RS is beneficial in adsorption and dispersion in hydrophobic environments.[23] Furthermore, compared with the size of RS particles (Fig. 3c), the diameter of IIP@RS (Fig. 3d) was significantly greater. These results confirmed that the imprinted layer was successfully coated onto RS particles during the Cd(ɪɪ) induced-Stöber process.

3.1.4 Contact angle analysis of IIP@RS.
The hydrophobic/hydrophilic nature of IIP@RS and RS particles was investigated by the contact angle technique. As shown in Fig. 3c, the θ value of 41.8° for RS particle was due to the presence of hydrophilic hydroxyl groups on its surface. After imprinting, the θ value of IIP@RS was increased to 141.8° (Fig. 3d). Generally, solid surfaces can be classified as super-hydrophobic ($\theta > 150°$), hydrophobic ($90° < \theta < 150°$), hydrophilic ($10° < \theta < 90°$) and super hydrophilic ($\theta < 10°$) based on their measured θ values.[24] The θ value of IIP@RS is very close to 150° (*i.e.* the critical value of super-hydrophobic materials), indicating that the imprinted film formed onto the RS particle surface possesses highly hydrophobic characteristics as expected. The high hydrophobicity of IIP@RS is beneficial in their adsorption ability toward Cd(ɪɪ) in hydrophobic vegetable oils. The increase in the contact angle value from 41.8° for RS particles to 141.8° for IIP@RS is mainly attributed to the hydrophobic-imprinted layer coated on RS particles.

3.2 The adsorption characteristics of IIP@RS

3.2.1 Effect of solvent type on adsorption kinetics of IIP@RS.
The nature of the solvent used in the binding process
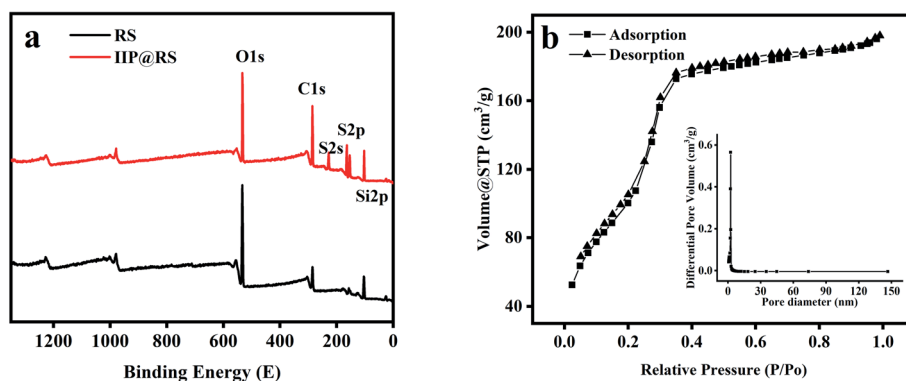

Fig. 2 XPS spectra (a), N$_2$ adsorption–desorption isotherms and size distribution (b) of IIP@RS.
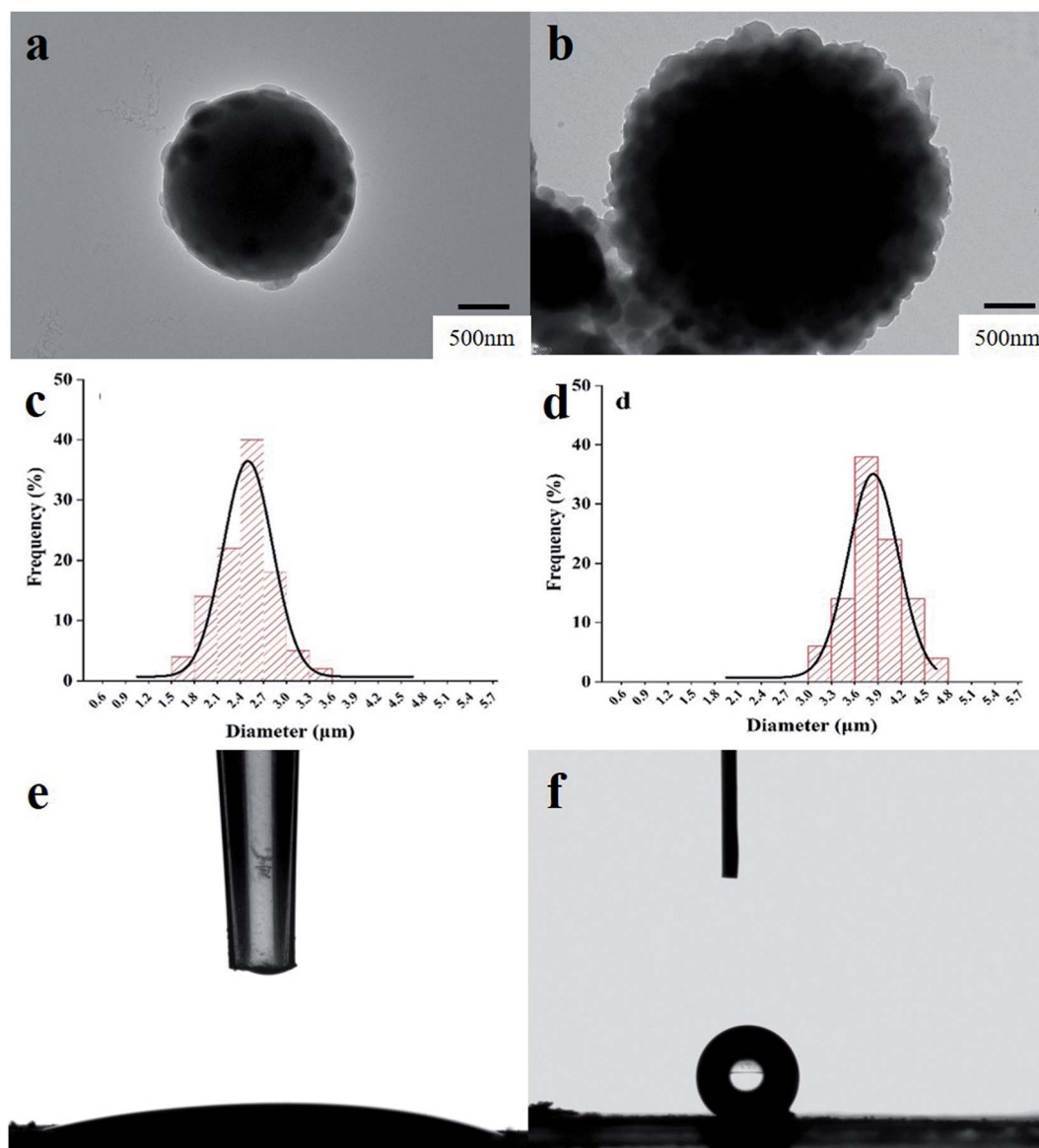
Fig. 3   TEM images of RS (a) and IIP@RS (b); particle size histogram of RS (c) and IIP@RS (d); contact angle analysis of RS (e) and IIP@RS (f).

can substantially influence the adsorption and recognition characteristics of IIPs.[25,26] Therefore, considering the solubility of Cd(II), the adsorption performance of IIP@RS in three solvents—water, ethanol and methanol—was investigated in this study. As shown in Fig. 4a, a high adsorption capability was achieved using ethanol as the adsorption solvent, while a low holding capacity was attained using water and methanol as the adsorption solvent. This is consistent with the better dispersibility of IIP@RS in ethanol compared with water and methanol. It is clear that solvents similar to the one used during the synthesis of IIP@RS favor the specific adsorption of Cd(II) on IIP@RS. This may be due to the mechanism of Cd(II) recognition by IIP@RS that mainly depends on two factors; (i) the shape of the imprinted cavity formed during the polymerization stage, and (ii) the spatial positioning of the functional groups coordinated with template ions in the imprinted cavity.[26] When

exposed to an improper solvent, the shrinking/swelling processes of imprinted polymers could affect the shape of the imprinted cavity and the distance between functional groups (–SH) in IIP@RS, and then decreased their recognition ability and adsorption rate toward the target ions.

The time required to reach equilibrium is a crucial parameter for the adsorption performance evaluation of sorbents. Therefore, the adsorption kinetics of IIP@RS toward Cd(II) in different solvents was investigated. In ethanol, the adsorption rate of IIP@RS and NIP@RS toward Cd(II) increased rapidly during the first 20 min due to a large number of available active sites for Cd(II) adsorption (Fig. 4b). In the following 10 min, the adsorption capacity increased at a slower rate and then reached a plateau due to the complete occupation of available specific binding sites. The adsorption kinetic curve of MIP@RS in methanol is similar to that in ethanol except for its low
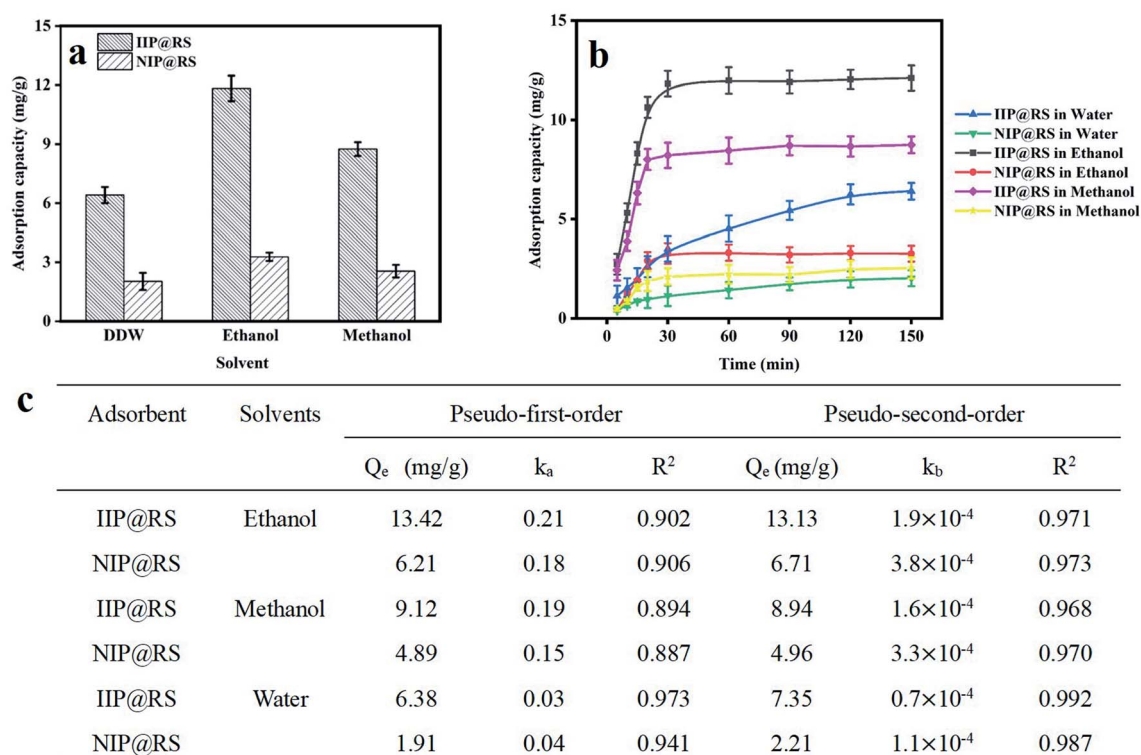
Fig. 4 The effect of solvent type (a) and contact time (b) on the adsorption characteristics of IIP@RS and NIP@RS; kinetic parameters of pseudo-first-order and pseudo-second-order models for adsorption of Cd(II) on IIP@RS and NIP@RS (c).

Adsorbent	Solvents	Pseudo-first-order			Pseudo-second-order		
		Q_e (mg/g)	k_a	R^2	Q_e (mg/g)	k_b	R^2
IIP@RS	Ethanol	13.42	0.21	0.902	13.13	1.9×10^{-4}	0.971
NIP@RS		6.21	0.18	0.906	6.71	3.8×10^{-4}	0.973
IIP@RS	Methanol	9.12	0.19	0.894	8.94	1.6×10^{-4}	0.968
NIP@RS		4.89	0.15	0.887	4.96	3.3×10^{-4}	0.970
IIP@RS	Water	6.38	0.03	0.973	7.35	0.7×10^{-4}	0.992
NIP@RS		1.91	0.04	0.941	2.21	1.1×10^{-4}	0.987

saturated adsorption capacity. Whereas, in water, the equilibrium adsorption of IIP@RS to Cd(II) was achieved in about 120 min. These results further confirmed that solvents similar to the one used during the synthesis of IIP@RS can significantly improve the affinity ability of imprinted sites of IIP@RS toward Cd(II) and enhance the geometric matching between Cd(II) and imprinted cavities.

Pseudo-first-order and pseudo-second-order equations were employed to analyze the potential rate-limiting steps of IIP@RS binding to Cd(II). The kinetic parameters and correlation coefficients are summarized in Fig. 4c. It was found that the goodness-of-fit of the pseudo-second-order equation for the experimental results was better than that of the pseudo-first-order equation. The higher correlation coefficient values obtained from the pseudo-second-order equation indicate that chemical adsorption *via* the coordination of Cd(II) to functional groups on IIP@RS is the rate-limiting step of the reaction.[27] The rate constants (k_a, k_b) of IIP@RS binding to Cd(II) in ethanol were also higher than those in water and methanol. It is, therefore, reasonable to deduce that the smaller diffusion barrier in ethanol can allow Cd(II) to quickly enter the imprinted cavities of IIP@RS.

3.2.2 **Adsorption isotherm.** The effect of the initial Cd(II) concentration on the adsorption capacity of IIP@RS was investigated in this study. As shown in Fig. 5a, the amount of Cd(II) adsorbed by IIP@RS increases rapidly when the initial concentration of Cd(II) ranged from 0 to 300 mg L^{-1}. With further increases in Cd(II) concentration, the amount of Cd(II)

adsorbed by the IIP@RS increased slowly until it reached a plateau. The maximum adsorption capacity of IIP@RS for Cd(II) was found to be 36.62 mg g^{-1}, but the maximum adsorption amount of Cd(II) on NIP@RS was only 8.43 mg g^{-1}, indicating an excellent selectivity (imprinting factor = 4.31) of IIP@RS towards Cd(II).

Freundlich and Langmuir isotherm models were used to describe the binding behavior of Cd(II) onto IIP@RS (Fig. 5b). The Langmuir model was found to be a good fit for the adsorption isotherm with a correlation coefficient of 0.996. The Langmuir adsorption isotherm is a monolayer adsorption model that assumes that the affinity ability of all binding sites is equivalent.[28] Thus, the distribution of binding sites for the IIP@RS binding to Cd(II) was homogenous, with monolayer adsorption. Moreover, the theoretical adsorption capacities of IIP@RS (42.63 mg g^{-1}) and NIP@RS (13.62 mg g^{-1}) calculated by the Langmuir model were close to their experimental binding capacities.

3.2.3 **Selective adsorption of Cd(II) on IIP@RS.** The specific recognition ability of IIP@RS and NIP@RS towards Cd(II) was investigated by employing Ni(II), Pb(II), Cr(II), and Cu(II) as competitor ions. It was found that the imprinting factors of IIP@RS for Cd(II), Ni(II), Pb(II), Cr(II), and Cu(II) were 3.73, 1.05, 1.03, 1.06, and 1.14, respectively. The selectivity factors of IIP@RS for Cd(II)/M(II) (M = Ni(II), Cr(II), Pb(II), and Cu(II)) were 3.54, 3.52, 3.62, and 3.28, respectively (Fig. 6). Clearly, IIP@RS exhibited a higher specific recognition ability to Cd(II) than other ions, despite their similar charge. These results further
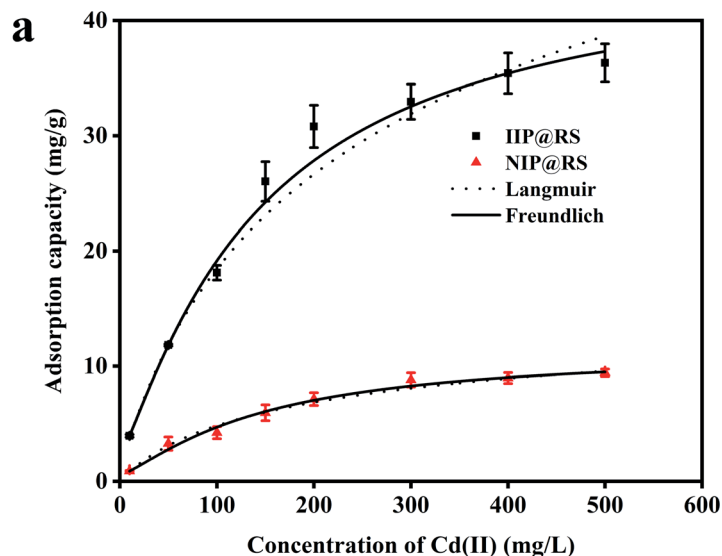
Fig. 5 The effect of the initial concentration of Cd(II) on the adsorption capacity of IIP@RS and NIP@RS (a), and the Langmuir and Freundlich adsorption isotherms parameters curve of IIP@RS and NIP@RS (b).

Adsorbents	Q_e (mg/g)	Langmuir model			Freundlich model			
		Q_{max} (mg/g)	K_L	R^2	Q_{max} (mg/g)	K_F	R^2	$1/n$
IIP@RS	36.62	42.63	0.0023	0.996	40.92	1.55	0.990	0.492
NIP@RS	8.43	13.62	0.0013	0.991	13.16	1.34	0.985	0.313

demonstrated that recognition cavities were successfully fabricated on the surface of IIP@RS during the polymerization process.
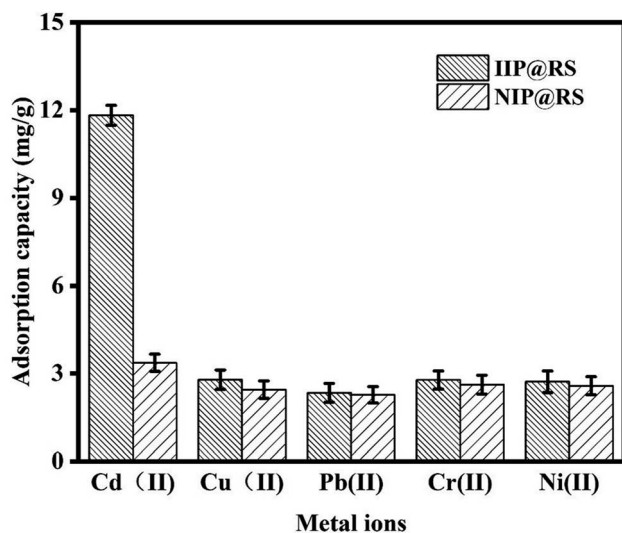

Fig. 6 The selective adsorption properties of the IIP@RS and NIP@RS toward Cd(II) with Cu(II), Pb(II), Cr(II), and Ni(II) as competitor ions.

3.3 Analytical performance

IIP@RS was loaded onto an IIP@IR-SPE column to enrich Cd(II) in real soybean oil, sunflower seed oil, corn oil, and olive oil samples. The retained Cd(II) in the SPE column was eluted and then determined by FAAS. It was observed that approximately 96.5–115.8% of Cd(II) was recovered from oil samples by this adsorption process with an RSD of 0.47–7.45% (Table 1). The high hydrophobic characteristics of IIP@RS could explain their excellent adsorption ability toward Cd(II) in hydrophobic vegetable oils. The calibration curve resulting from the proposed method was

Table 1 The analysis results of Cd(II) ions in four spiked oil samples ($n = 3$)

Samples	Added (mg L^{-1})	Found (mg L^{-1})	Recovery (%)	RSD (%)
Soybean oil	2	1.96	98.0	3.41
	10	11.47	114.7	1.65
Sunflower seed oil	2	2.06	103	4.40
	10	11.58	115.8	0.47
Corn oil	2	2.07	103.5	4.40
	10	11.17	111.7	3.53
Olive oil	2	1.93	96.5	2.12
	10	10.04	100.4	7.45

Table 2 Comparison with other adsorbents

Monomer	Template	Maximum adsorption capacity (mg g^{-1})	Equilibrium time (min)	Imprinting factor	Reference
(3-Mercaptopropyl)trimethoxysilane	Cd(II)	4.8	30	6	29
Afford aminoethyl chitosan	Cd(II)	26.1	60	3.8	30
Methacrylic acid–acrylamide	Cd(II)	46.8	36	3.1	31
Allyl thiourea	Cd(II)	38.3	9	2.8	32
N-[(3-Trimethoxysilyl)propyl]ethylenediamine triacetic acid trisodium salt	Cd(II)	18.18	18	11.9	33
(3-Mercaptopropyl)trimethoxysilane	Cd(II)	5.26	60	4.12	34
3-[2-(2-Aminoethylamino)ethylamino]propyltrimethoxysilane	Cd(II)	24.7	30	2.02	35
3-(γ-Aminoethylamino)propyltrimethoxysilane	Cd(II)	40	120	3	36
(3-Mercaptopropyl)trimethoxysilane	Cd(II)	32.9	24	2.9	37
(3-Mercaptopropyl)trimethoxysilane	Cd(II)	17.57	30	2.1	38
(3-Mercaptopropyl)trimethoxysilane	Cd(II)	36.62	30	4.31	This work

linear with a correlation coefficient of 0.9923, a detection limit of 0.62 µg L^{-1} (S/N = 3), and a quantitation limit of 1.81 µg L^{-1}. Adsorption–desorption cycling tests were further performed to investigate the potential recyclability and stability of the IIP@RS-SPE system. It was found that the recovery of Cd(II) on the IIP@RS-SPE system remained above 93% after at least 6 cycles. These results illustrate that the proposed IIP@RS-SPE system in this work can be repeatedly used to enrich and analyze Cd(II) in complex vegetable oil samples.

3.4 Comparison with other adsorbents

A comparison of the maximum adsorption capacity, equilibrium time, and imprinting factor between different Cd(II)-imprinted polymers is presented in Table 2. It is clear that the

adsorption performance of IIP@RS toward Cd(II) was better than that of the majority of other imprinted polymers.[29–38]

3.5 The mechanism of IIP@RS binding to Cd(II)

Previously, the ITC method was used to analyze the binding thermodynamic characteristics of Cd(II) with the MPTMS and TMOS, the structures of which are very similar, the latter being deficient of a thiol (–SH) group. The results showed that the MPTMS binding to Cd(II) produced higher exothermic heat, whereas no significant reaction heat was observed for the binding of TMOS and Cd(II). Therefore, the thiol groups of the MPTMS molecules were considered to be the main imprinted sites that enabled coordination binding to Cd(II).[39] In this study, the thiol groups contents in IIP@RS, NIP@RS, and RS-SH were further investigated and then their adsorption amounts for
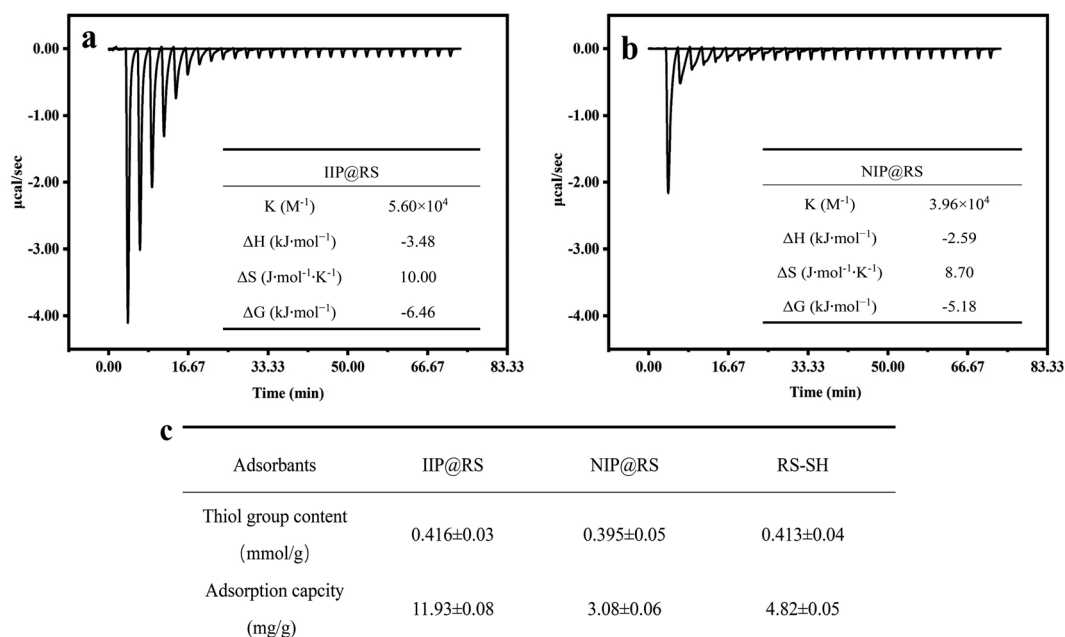

Fig. 7 Effect of thiol group content on the adsorption capacity of IIP@RS, NIP@RS and RS-SH (a); mechanism analysis of IIP@RS (b) and NIP@RS (c) binding to Cd(II) using ITC.

Cd(II) were compared. As shown in Fig. 7c, there were no significant differences in the thiol group content among IIP@RS, RS-SH, and NIP@RS. However, the adsorption capacity of IIP@RS to Cd(II) was significantly higher than that of RS-SH and NIP@RS. These results suggested that the Cd(II)-induced cavities during gel formation mainly attributed to the recognition behavior of IIP@RS toward Cd(II).[21,40]

The adsorption behavior of Cd(II) by IIP@RS and NIP@RS were analyzed using an ITC method to further explore their recognition mechanisms toward Cd(II). Similar to the binding behavior between Cd(II) and MPTMS, the adsorption process of Cd(II) by IIP@RS produced strong exothermic heat during the initial titration period. Then, the exothermic heat was quickly released and reached a stable state (Fig. 7a). In contrast, low exothermic heat was found during the titration of Cd(II) by NIP@RS (Fig. 7b). NIP@RS, obtained by applying the same polymerization procedure in the absence of the template Cd(II), possesses the same chemical properties as IIP@RS but without any specific cavities created during the polymerization step. Therefore, the results of ITC measurement further indicated that the recognition behavior of IIP@RS toward Cd(II) is a result of the spatial complementarities of the template ions and functional monomer in the imprinted cavities.

The titration experiments were fitted using an independent binding site model to attain the reaction enthalpy (ΔH), stability constant (K_{ITC}), and entropy (ΔS), which were then used to analyze the binding mechanism of IIP@RS to Cd(II).[41] As shown in Fig. 7a and b, the fit provided an enthalpy value of -3.48 kJ mol^{-1} and a high K_{ITC} value of 5.60×10^4 M^{-1}, indicating that IIP@RS possesses an excellent binding ability to capture and lock Cd(II) within the imprinted shape cavities *via* an exothermic process. The thermodynamic force driving the binding of IIP@RS and Cd(II) was investigated by observing ΔH and ΔS.[42] A positive entropy of 13.12 J mol^{-1} K^{-1} and negative enthalpy of -4.13 kJ mol^{-1} was obtained, which indicates that the adsorption process of IIP@RS toward Cd(II) is driven by both the entropy (ΔS) and enthalpy (ΔH). The ΔG (free energy) was also calculated according to $\Delta G = \Delta H - T\Delta S$, for which a negative value of -6.46 kJ mol^{-1} was obtained, demonstrating that the adsorption process of IIP@RS toward Cd(II) was spontaneous at any temperature.[43]

4 Conclusions

In this study, a novel ion-imprinting polymer was coated onto the surface of the RS particles for the selective extraction of Cd(II) from edible vegetable oils. The obtained IIP@RS exhibited high hydrophobicity with a large specific surface area and uniform porous structure. IIP@RS also possessed high adsorption capacity and excellent selectivity with a high equilibrium adsorption rate. Furthermore, the recognition behavior of IIP@RS to Cd(II) mainly contributes to the Cd(II)-induced cavities during gel formation and affinity with the thiol group of MPTMS in imprinted cavities. In real edible vegetable oils, IIP@RS-SPE can extract approximately 96.5–115.8% of Cd(II), suggesting that it has a broad potential for Cd(II) enrichment and determination from vegetable oils. In future research, the

actual sample analysis on a large scale will be conducted to achieve industrial applications of IIP@RS.

Ethical statement

This article does not contain any studies with human participants or animals conducted by any of the authors.

Conflicts of interest

All authors declare no conflict of interest.

References

1 X. Mao, A. Yan, Y. Wan, D. Luo and H. Yang, Dispersive Solid-Phase Extraction Using Microporous Sorbent UiO-66 Coupled to Gas Chromatography–Tandem Mass Spectrometry: A QuEChERS-Type Method for the Determination of Organophosphorus Pesticide Residues in Edible Vegetable Oils without Matrix Interference, *J. Agric. Food Chem.*, 2019, **67**, 1760–1770.

2 L. Yao, H. Liu, X. Wang, W. Xu, Y. Zhu, H. Wang, L. Pang and C. Lin, Ultrasound-assisted surfactant-enhanced emulsification microextraction using a magnetic ionic liquid coupled with micro-solid phase extraction for the determination of cadmium and lead in edible vegetable oils, *Food Chem.*, 2018, **256**, 212–218.

3 J. S. Almeida, T. A. Anunciação, G. C. Brandão, A. F. Dantas, V. A. Lemos and L. S. G. Teixeira, Ultrasound-assisted single-drop microextraction for the determination of cadmium in vegetable oils using high-resolution continuum source electrothermal atomic absorption spectrometry, *Spectrochim. Acta, Part B*, 2015, **107**, 159–163.

4 M. Karimi, S. Dadfarnia, A. M. H. Shabani, F. Tamaddon and D. Azadi, Deep eutectic liquid organic salt as a new solvent for liquid-phase microextraction and its application in ligandless extraction and preconcentraion of lead and cadmium in edible oils, *Talanta*, 2015, **144**, 648–654.

5 V. Modi, S. Akst and D. Davison, 1715: acute cadmium toxicity causing multisystem organ failure, *Crit. Care Med.*, 2019, **47**, 831.

6 A. Zhuravlev, A. Zacharia, S. Gucer, A. Chebotarev, M. Arabadji and A. Dobrynin, Direct atomic absorption spectrometry determination of arsenic, cadmium, copper, manganese, lead and zinc in vegetable oil and fat samples with graphite filter furnace atomizer, *J. Food Compos. Anal.*, 2015, **38**, 62–68.

7 I. López-García, Y. Vicente-Martínez and M. Hernández-Córdoba, Determination of cadmium and lead in edible oils by electrothermal atomic absorption spectrometry after

reverse dispersive liquid–liquid microextraction, *Talanta*, 2014, **124**, 106–110.

8 R. Ansari, T. G. Kazi, M. K. Jamali, M. B. Arain, M. D. Wagan, N. Jalbani, H. I. Afridi and A. Q. Shah, Variation in accumulation of heavy metals in different verities of sunflower seed oil with the aid of multivariate technique, *Food Chem.*, 2009, **115**, 318–323.

9 Z. Kowalewska, B. Izgi, S. Saracoglu and S. Gucer, Application of liquid-liquid extraction and adsorption on activated carbon to the determination of different forms of metals present in edible oils, *Chem. Anal.*, 2005, **50**, 1007.

10 I. S. Barreto, S. I. Andrade, F. A. Cunha, M. B. Lima, M. C. U. Araujo and L. F. Almeida, A robotic magnetic nanoparticle solid phase extraction system coupled to flow-batch analyzer and GFAAS for determination of trace cadmium in edible oils without external pretreatment, *Talanta*, 2018, **178**, 384–391.

11 X. Yu, Z. Li, M. Zhao, S. C. S. Lau, H. R. Tan, W. J. Teh, H. Yang, C. Zheng and Y. Zhang, Quantification of aflatoxin B1 in vegetable oils using low temperature clean-up followed by immuno-magnetic solid phase extraction, *Food Chem.*, 2019, **275**, 390–396.

12 V. Yilmaz, H. Yilmaz, Z. Arslan and J. Leszczynski, Novel imprinted polymer for the preconcentration of cadmium with determination by inductively coupled plasma mass spectrometry, *Anal. Lett.*, 2017, **50**, 482–499.

13 J. He, Y. Lu, T. Zhao and Y. Li, Preparation of polydopamine-coated, graphene oxide/Fe$_3$O$_4$-imprinted nanoparticles for selective removal of sulfonylurea herbicides in cereals, *J. Sci. Food Agric.*, 2020, **100**, 3822–3831.

14 H. Ashkenani and M. A. Taher, Determination of cadmium (II) using carbon paste electrode modified with a Cd-ion imprinted polymer, *Microchim. Acta*, 2012, **178**, 53–60.

15 M. Behbahani, M. Barati, M. K. Bojdi, A. R. Pourali, A. Bagheri and N. A. G. Tapeh, A nanosized cadmium (II)-imprinted polymer for use in selective trace determination of cadmium in complex matrices, *Microchim. Acta*, 2013, **180**, 1117–1125.

16 S. Liu, S. S. Latthe, H. Yang, B. Liu and R. Xing, Raspberry-like superhydrophobic silica coatings with self-cleaning properties, *Ceram. Int.*, 2015, **41**, 11719–11725.

17 C. Du, N. Zhang, S. Ding, X. Gao, P. Guan and X. Hu, Preparation of highly cross-linked raspberry-like nano/microspheres and surface tailoring for controlled immunostimulating peptide adsorption, *Polym. Chem.*, 2016, **7**, 4531–4541.

18 M. Yu, Q. Wang, M. Zhang, Q. Deng and D. Chen, Facile fabrication of raspberry-like composite microspheres for the construction of superhydrophobic films and applications in highly efficient oil–water separation, *RSC Adv.*, 2017, **7**, 39471–39479.

19 X. Xu, M. Wang, Q. Wu, Z. Xu and X. Tian, Synthesis and application of novel magnetic ion-imprinted polymers for selective solid phase extraction of cadmium (II), *Polymers*, 2017, **9**, 360.

20 G. Bulaj, T. Kortemme and D. P. Goldenberg, Ionization–reactivity relationships for cysteine thiols in polypeptides, *Biochemistry*, 1998, **37**, 8965–8972.

21 Y. S. Minaberry and M. Tudino, An ion imprinted amino-functionalized mesoporous sorbent for the selective minicolumn preconcentration of cadmium ions and determination by GFAAS, *Anal. Methods*, 2018, **10**, 5305–5312.

22 Y. Liu, Z. Liu, Y. Wang, J. Dai, J. Gao, J. Xie and Y. Yan, A surface ion-imprinted mesoporous sorbent for separation and determination of Pb (II) ion by flame atomic absorption spectrometry, *Microchim. Acta*, 2011, **172**, 309–317.

23 X. Zou, C. Tao, K. Yang, F. Yang, H. Lv, L. Yan, H. Yan, Y. Li, Y. Xie and X. Yuan, Rational design and fabrication of highly transparent, flexible, and thermally stable superhydrophobic coatings from raspberry-like hollow silica nanoparticles, *Appl. Surf. Sci.*, 2018, **440**, 700–711.

24 M. Iqbal, D. K. Dinh, Q. Abbas, M. Imran, H. Sattar and A. Ul Ahmad, Controlled surface wettability by plasma polymer surface modification, *Surfaces*, 2019, **2**, 349–371.

25 T. Pap, V. Horváth, A. Tolokán, G. Horvai and B. Sellergren, Effect of solvents on the selectivity of terbutylazine imprinted polymer sorbents used in solid-phase extraction, *J. Chromatogr. A*, 2002, **973**, 1–12.

26 N. W. Turner, E. V. Piletska, K. Karim, M. Whitcombe, M. Malecha, N. Magan, C. Baggiani and S. A. Piletsky, Effect of the solvent on recognition properties of molecularly imprinted polymer specific for ochratoxin A, *Biosens. Bioelectron.*, 2004, **20**, 1060–1067.

27 Y. Huang, T. Zhao and J. He, Preparation of magnetic molecularly imprinted polymers for the rapid detection of diethylstilbestrol in milk samples, *J. Sci. Food Agric.*, 2019, **99**, 4452–4459.

28 W. Yang, D. Niu, X. Ni, Z. Zhou, W. Xu and W. Huang, Core–Shell Magnetic Molecularly Imprinted Polymer Prepared for Selectively Removed Indole from Fuel Oil, *Adv. Polym. Technol.*, 2017, **36**, 168–176.

29 Y. Miao, H. Zhang, Q. Xie and N. Chen, Construction and selective removal of Cd ion based on diatom-based Cd (II) ion-imprinted composite adsorbent, *Colloids Surf., A*, 2020, **598**, 124856.

30 H. Wang, *et al.*, A Novel Magnetic Cd(II) Ion-Imprinted Polymer as a Selective Sorbent for the Removal of Cadmium Ions from Aqueous Solution, *J. Inorg. Organomet. Polym. Mater.*, 2019, **29**, 1874–1885.

31 X. Xu, M. Wang, Q. Wu, Z. Xu and X. Tian, Synthesis and Application of Novel Magnetic Ion-Imprinted Polymers for Selective Solid Phase Extraction of Cadmium (II), *Polymers*, 2017, **9**, 360.

32 M. Li, *et al.*, Synthesis and characterization of a surface-grafted Cd(II) ion-imprinted polymer for selective separation of Cd(II) ion from aqueous solution, *Appl. Surf. Sci.*, 2015, **332**, 463–472.

33 M. Fattahi, *et al.*, Micro solid phase extraction of cadmium and lead on a new ion-imprinted hierarchical mesoporous polymer via dual-template method in river water and fish

muscles: optimization by experimental design, *J. Hazard. Mater.*, 2021, **403**, 123716.

34 L. Huang, *et al.*, Preparation, characterization and adsorption characteristics of diatom-based Cd(II) surface ion-imprinted polymer, *J. Dispersion Sci. Technol.*, 2020, 1–12.

35 M. Ghanei-Motlagh and M. A. Taher, Novel imprinted polymeric nanoparticles prepared by sol–gel technique for electrochemical detection of toxic cadmium(II) ions, *Chem. Eng. J.*, 2017, **327**, 135–141.

36 W. Li, *et al.*, One-step synthesis of periodic ion imprinted mesoporous silica particles for highly specific removal of Cd^{2+} from mine wastewater, *J. Sol-Gel Sci. Technol.*, 2016, **78**, 632–640.

37 B. Zhao, *et al.*, Novel ion imprinted magnetic mesoporous silica for selective magnetic solid phase extraction of trace Cd followed by graphite furnace atomic absorption spectrometry detection, *Spectrochim. Acta, Part B*, 2015, **107**, 115–124.

38 X. Luo, *et al.*, Synthesis of magnetic ion-imprinted fluorescent CdTe quantum dots by chemical etching and their visualization application for selective removal of Cd(II) from water, *Colloids Surf., A*, 2014, **462**, 186–193.

39 P. Yang, H. Cao, D. Mai, T. Ye, X. Wu, M. Yuan, J. Yu and F. Xu, A novel morphological ion imprinted polymers for selective solid phase extraction of Cd(II): preparation, adsorption properties and binding mechanism to Cd(II), *React. Funct. Polym.*, 2020, **151**, 104569.

40 S. Nagappan, H. M. Ha, S. S. Park, N.-J. Jo and C.-S. Ha, One-pot synthesis of multi-functional magnetite–polysilsesquioxane hybrid nanoparticles for the selective Fe 3+ and some heavy metal ions adsorption, *RSC Adv.*, 2017, **7**, 19106–19116.

41 T. Yilmaz, L. Maldonado, H. Turasan and J. Kokini, Thermodynamic mechanism of particulation of sodium alginate and chitosan polyelectrolyte complexes as a function of charge ratio and order of addition, *J. Food Eng.*, 2019, **254**, 42–50.

42 M. Li, S. A. Messele, Y. Boluk and M. G. El-Din, Isolated cellulose nanofibers for Cu (II) and Zn (II) removal: performance and mechanisms, *Carbohydr. Polym.*, 2019, **221**, 231–241.

43 H. Du, C. Qu, M. Ma, M. Lei, B. Tie, X. Liu, X. Wei and Y. Yang, Insights into Pb(II) binding by Fe/Al hydroxide–microbe composite: XAFS spectroscopy and isothermal titration calorimetry study, *Chem. Geol.*, 2019, **510**, 84–90.